

Internal and External Leakage Current Decomposition of Surge Arresters Using Discrete Fourier Transform



Tamadher Almomani¹, E. A. Feilat², I.A. Metwally³

¹Al-Balqa Applied University, tamaduralmomani@bau.edu.jo

²The University of Jordan, Jordan, e.feilat@ju.edu.jo

³Sultan Qaboos University, Oman, metwally@squ.edu.om

ABSTRACT

Surge arresters are over voltage protection devices that provide protection to power transmission and distribution systems from over voltages caused by lightning surges, switching operations in power systems and temporary over voltages caused by faults. However, they are subjected to aging due to environmental conditions and overheating. Therefore to avoid catastrophic failures of surge arresters, it is necessary to evaluate their performance either by online monitoring or offline testing of the resistive leakage current which is considered as one of most techniques for assessing the degradation level of surge arresters. This paper presents an efficient technique for decomposition of leakage currents of surge arresters using discrete Fourier transform. The paper aims to decompose the leakage current, either internal or external, into its resistive and capacitive components. After separating the two current components, the third harmonic resistive current, which is considered an important indicator of SA degradation, is extracted from the resistive current component. In this paper, diagnosis of three different 33 kV, 10 kA distribution-class surge arresters, namely Zinc Oxide Polymeric-, Zinc Oxide Silicon Rubber- and Silicon Carbide Porcelain-housed surge arresters is presented. Both the internal and the external currents were measured for each arrester up to its maximum continuous operating voltage.

Key words: Aging, arrester, Fourier transform, leakage current, monitoring.

1. INTRODUCTION

Transmission and distribution overhead lines are usually protected against over voltages caused by lightning and switching surges as well as temporary over voltages [1]–[4]. One of the most effective and in-expensive ways to protect the transmission line from lightning overvoltage is by installing either Silicon Carbide (SiC) surge arresters (SAs) with spark gaps, SiC SAs with current limiting gaps and gapless Zinc Oxide (ZnO) SAs. Their function is to limit the

magnitude of over voltages to a safe acceptable level below the basic insulation level (BIL) of equipment being protected by absorbing and dissipating its energy [5].

The SiC SA has some superior electrical characteristics. It has a very high nonlinear resistance under low voltage condition, but a very low resistance to high voltage conduction [5]–[6]. When an over voltage occurs, the SiC resistance breaks down allowing conduction of the internal leakage current (ILC) to ground. However, SiC SAs have some disadvantages that make it undesirable as an over voltage protection device as the SiC blocks are vulnerable to moisture; therefore it was replaced by ZnO SAs [7]. The ZnO SA is an arrester that is commonly used today's in power system over voltage protection. Unlike SiC SAs, the ZnO SAs have no airgaps (gapless) and therefore eliminate the heat associated with arcing discharges and offer more excellent characteristics [8]. Gapped arresters are not able to limit the switching overvoltage effectively. Therefore, the gapless ZnO SAs which exhibit high nonlinear voltage current (V-I) characteristics and faster conduction response for over voltage surges are developed [9]–[11]. The SiC SAs have been replaced by ZnO arresters but a large number of SiC arresters are still operating and in service [6].

Over the past years researchers have conducted many research studies related to aging and degradation of SAs by developing online and offline based monitoring techniques and indicators. Many methods for the determination of arresters' conditions have been presented such as V-I characteristic curve analysis [7], partial discharge and electromagnetic radiation measurement [12]–[13], ultrasonic and radio interference detection [14] and certainly the leakage current (LC) measurement where, the majority of diagnostic methods are based on the total leakage current (TLC) magnitude and harmonics measurements [15]–[32].

As a result of several investigations, it was noticed that the TLC of a SA was used for condition monitoring [15]–[26]. Furthermore, other research studies showed that the resistive component of TLC can be indicative about the level of arrester

deterioration. Consequently, several monitoring techniques which include modified shifted current, current orthogonality, field probe method and capacitive current compensation techniques were developed to accurately monitor and extract the resistive current component [1], [15]–[16], [27]–[32]. Moreover, some research studies focused on monitoring the third harmonic component of resistive leakage current (RLC) as a good aging indicator due to the strong relationship between SA aging and the level of third harmonic component [27]–[31]. This will be the main concern of this paper as developing a technique for monitoring the LC and extracting the third harmonic current is therefore, important to maintain reliability, economy, performance, and continuity of power system operation.

Online measurement techniques give fast assessment on the condition of SAs and can be used for the predictive maintenance. However, the disadvantage of online monitoring technique is that the measurement of the TLC is influenced by voltage harmonics. On the other hand, offline measurement techniques can be applied using voltage source that are suited for this purpose, the offline methods therefore have good accuracy [33].

In previous research works, the TLC combining the ILC and external leakage currents (ELC) were examined. In this paper a simple yet efficient offline technique for decomposition of the LC using discrete Fourier transform (DFT) is presented. The paper aims to decompose the LC, either ILC or ELC, into its resistive and capacitive components. After, separating the two current components, the third harmonic resistive current is extracted from the resistive current component. Three different 33 kV-10 kA distribution-class surge arresters, namely Zinc Oxide (ZnO) polymeric-, ZnO Silicon rubber (SiR)- and Silicon Carbide (SiC) Porcelain-housed SAs are tested. Both of the two ZnO SAs are new whereas the SiC SA is an aged one (15 years in service). Both the ILC and the ELC were measured for each SA up to its maximum continuous operating voltage (MCOV) [27]. The specifications of the SAs are provided the Appendix [27]. Matlab software has been used for analyzing the measured ILC and ELC signals.

2. EQUIVALENT CIRCUIT OF SURGE ARRESTER

A SA has high voltage and ground terminals and usually installed between phase and earth/neutral. Under normal operating conditions, the SA acts as an insulator, however, when get subjected to a transient over voltage greater than normal line voltage, the SA provides a low impedance path to ground and hence diverts the current through the semiconductor blocks to ground thus limiting the over voltage and avoid equipment damage or service interruption and then restore back to a normal condition. This current is called ILC. In addition, some current leaks to ground through the housing insulation, this is called ELC [9-11].

The SA is modeled by an equivalent circuit consistent of capacitive branch in parallel with a non-linear resistive branch as shown in Figure 1. Thus, the ILC or ELC of a SA comprises two components, namely capacitive component originated from the metal permittivity of the SA and the resistive component due to intrinsic resistance of the semiconductor blocks [15-21].

Practically, capacitive leakage current (CLC) component does not change. Therefore it is not important in the monitoring. On the contrary, the resistive leakage current (RLC) component varies with changes in SA characteristics, operating voltage, ambient temperature, lightning current discharge, and environmental factors. Accordingly, the RLC can give a good indicator of SA aging. Moreover, because of the nonlinear V-I characteristics of the SA, the RLC component implies odd harmonic current components that may cause overheating, deterioration and failure of SAs. In particular, the third harmonic current component has a strong relationship with aging. Therefore, it is considered the most important indicator of SA aging [19-26].

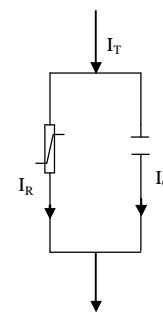


Figure 1: Equivalent Circuit of Surge Arrester

2.1 Mathematical Analysis

The ILC and ELC can be expressed as a sum of the capacitive and resistive current components as follows:

$$i_i(t) = i_{Ci}(t) + i_{Ri}(t) \tag{1}$$

$$i_e(t) = i_{Ce}(t) + i_{Re}(t)$$

where $i_i(t)$ and $i_e(t)$ are the measured ILC and ELC, respectively. Similarly, $i_{Ci}(t)$, $i_{Ri}(t)$, $i_{Ce}(t)$, and $i_{Re}(t)$ are the internal and external capacitive and resistive current components, respectively. $i_r(t)$ is the resistive current component including odd harmonics.

In offline leakage current measurements, the tests are usually conducted in a high voltage laboratory using high voltage AC source. The voltage source is used to generate a pure sinusoidal voltage $v(t)$. Assume that $v(t) = V_m \sin(\omega t)$, the capacitive current $i_c(t)$ contains the fundamental component which is orthogonal to the applied voltage waveform, $i_c(t) = Cdv(t)/dt$, whereas resistive current $i_r(t)$ is in phase with the applied voltage waveform and includes odd harmonics. Accordingly, the ILC or ELC can be expressed as

$$i_i(t) = I_{Ci1} \cos(\omega t) + \sum_k I_{Rik} \sin(k\omega t)$$

$$i_e(t) = I_{Ce1} \cos(\omega t) + \sum_k I_{Rek} \sin(k\omega t)$$
(2)

where I_{Ci1} or I_{Ce1} is the peak value of the fundamental CLC and I_{Rik} or I_{Rek} is the peak value of the k^{th} harmonic RLC. Usually, the third harmonic resistive current is the dominant harmonic component.

2.2 Proposed Technique

In this work, the measured ILC and ELC and their associated harmonic spectrums for an MCOV voltage reference signal are measured. Using Fourier series expansion for a periodic waveform, the ILC and ELC waveforms can be expanded as

$$i_i(t) = \sum_k a_{ki} \cos(k\omega t) + \sum_k b_{ki} \sin(k\omega t)$$

$$i_e(t) = \sum_k a_{ke} \cos(k\omega t) + \sum_k b_{ke} \sin(k\omega t)$$
(3)

where a_{ki} , b_{ki} , a_{ke} , and b_{ke} are the real and imaginary Fourier coefficients of ILC and ELC waveforms. These coefficients can be calculated using discrete Fourier transform (DFT). For N samples of one cycle of the measured ILC or ELC $i_i(n)=\{i_{i0}, i_{i1}, \dots, i_{iN-1}\}$ and $i_e(n)=\{i_{e0}, i_{e1}, \dots, i_{eN-1}\}$, the Fourier coefficients of are calculated as

$$a_{ki/e} = \frac{2}{N} \sum_{n=0}^{N-1} i_{i/en} \cos\left(\frac{2\pi kn}{N}\right)$$

$$b_{ki/e} = \frac{2}{N} \sum_{n=0}^{N-1} i_{i/en} \sin\left(\frac{2\pi kn}{N}\right)$$
(4)

Considering the voltage waveform as a reference signal and comparing equations (2) and (3), one concludes that a_{ki} , b_{ki} , a_{ke} , and b_{ke} coefficients represent the k^{th} peak values of the capacitive and the resistive harmonic current components, respectively. Next, after calculating the Fourier coefficients, the internal or external capacitive current $i_{Ci/e}(t)$ and the resistive current $i_{Ri/e}(t)$ can be constructed as follows. If voltage source harmonics are negligible, then $i_{Ci/e}(t)$ and $i_{Ri/e}(t)$ can be obtained as follows.

$$i_{Ci}(t) = \sum_k a_{ki} \cos(k\omega t) \cong a_{i1} \cos(\omega t)$$

$$i_{Ri}(t) = \sum_k b_{ki} \sin(k\omega t) = b_{i1} \sin(\omega t) + b_{i3} \sin(3\omega t) + \dots$$
(5)

$$i_{Ce}(t) = \sum_k a_{ke} \cos(k\omega t) \cong a_{e1} \cos(\omega t)$$

$$i_{Re}(t) = \sum_k b_{ke} \sin(k\omega t) = b_{e1} \sin(\omega t) + b_{e3} \sin(3\omega t) + \dots$$
(6)

The approximation given in (5) and (6) is highly applicable for ZnO SAs

3. EXPERIMENTAL SETUP

The experimental arrangement for measuring the ILC and ELC of the tested SAs is shown in Fig. 2. A 240V/400kV, 200

kVA, 50 Hz high-voltage transformer was used. The SA was directly connected to the high voltage terminal of the transformer. A capacitive voltage divider with a ratio of 7:1 in addition to an AC peak voltmeter was used to measure the applied voltage. The ILC and ELC ($i_i(t)$ and $i_e(t)$) were measured using two shunt resistors of 1 kΩ and 100 kΩ, respectively. The voltage waveform was considered as reference signal. The ILC was separated from the housing ELC by applying a grease layer near the base of the SA as indicated in Figure 2 [27].

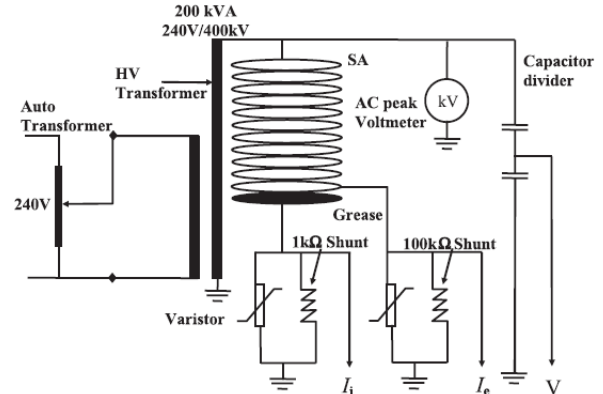
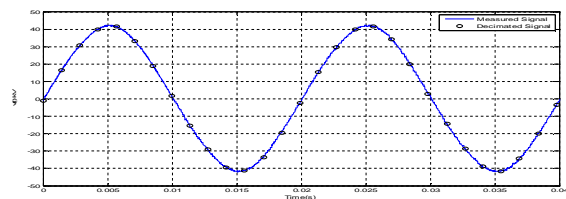


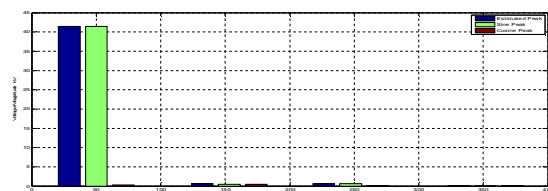
Figure 2: Test Circuit for the Measurement of both Internal and External Total Leakage Currents

4. RESULTS AND DISCUSSION

In this work, three different SAs were tested at an MCOV of 29 kV_{rms} for extracting the ILC and ELC and their corresponding harmonic components. The voltage, ILC and ELC signals were captured and stored by a digital storage oscilloscope in the *.CSV file form. The Matlab software was used for signal decomposition and harmonic estimation. Figure 3 shows the applied voltage waveform and its corresponding harmonic spectrum. It can be seen that the voltage is almost pure sinusoid with negligible harmonics.



(a) Voltage Waveform



(b) Voltage Harmonic Spectrum

Figure 3: Applied Voltage Waveform and Harmonic Spectrum The measured ILC and ELC of the three tested SAs are displayed in Figure 4.

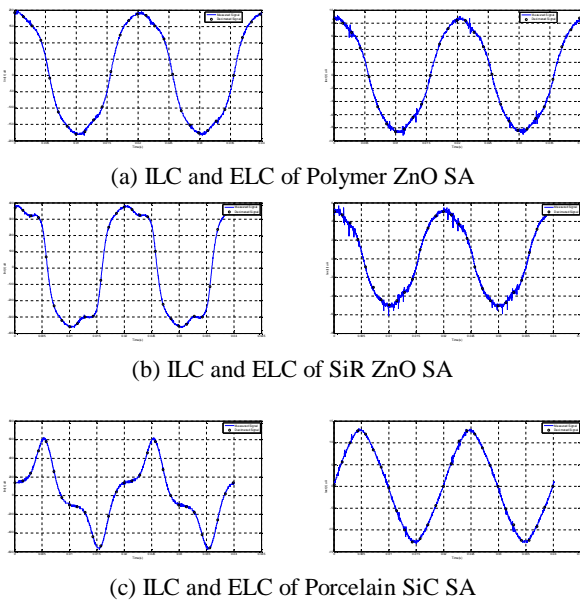


Figure 4: Internal and External Leakage Currents of Tested SAs

The current decomposition of the ILC and ELC of the three tested SAs into capacitive and resistive components are depicted in Figure 5.

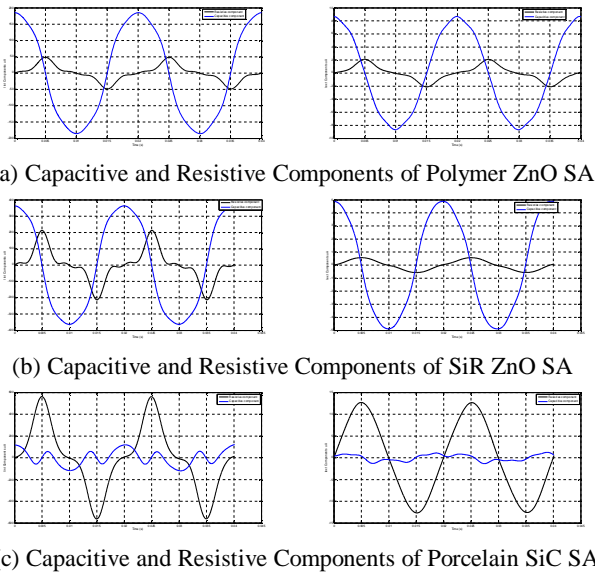
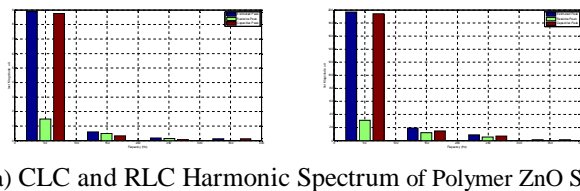


Figure 5: Capacitive and Resistive Current Components of the Internal and External Leakage Currents of Tested SAs

The harmonic spectrum of the CLC and RLC components for the tested SAs are illustrated in Figure 6.



(a) CLC and RLC Harmonic Spectrum of Polymer ZnO SA

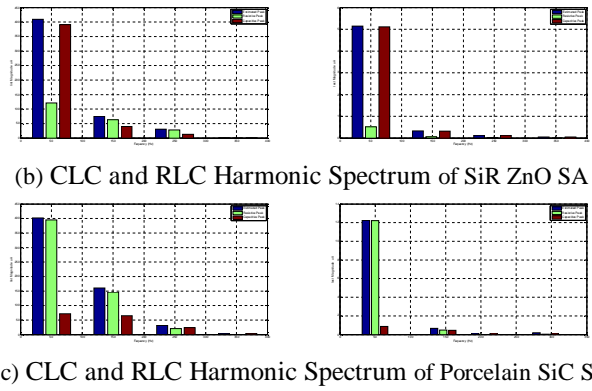


Figure 6: Harmonic Spectrum of the Capacitive and Resistive Internal and External Leakage currents of the Tested SAs

Table 1: Peak values of the internal and external leakage currents and their capacitive and resistive components of Polymer ZnO SA

Harmonic Order	Total Peak (μA)		Capacitive Peak (μA)		Resistive Peak (μA)	
	I_{int}	I_{ext}	I_{int}	I_{ext}	I_{int}	I_{ext}
1	196.7	8.88	194.3	8.77	30.94	1.49
3	19.13	0.59	14.77	0.33	12.15	0.49
5	8.66	0.17	6.78	0.11	5.38	0.14
7	1.14	0.13	1.14	0.13	0.00	0.00

Table 2: Peak values of the internal and external leakage currents and their capacitive and resistive components of SiR ZnO SA

Harmonic Order	Total Peak (μA)		Capacitive Peak (μA)		Resistive Peak (μA)	
	I_{int}	I_{ext}	I_{int}	I_{ext}	I_{int}	I_{ext}
1	409.5	5.14	391.1	5.11	121.3	0.52
3	74.81	0.32	40.03	0.32	63.19	0.06
5	30.89	0.13	12.21	0.13	28.11	0.01
7	0.74	0.048	0.74	0.048	0.00	0.00

Table 3: Peak values of the internal and external leakage currents and their capacitive and resistive components of Porcelain SiC SA

Harmonic Order	Total Peak (μA)		Capacitive Peak (μA)		Resistive Peak (μA)	
	I_{int}	I_{ext}	I_{int}	I_{ext}	I_{int}	I_{ext}
1	401.8	12.25	71.74	0.885	395.3	12.21
3	160.2	0.67	64.69	0.463	146.5	0.483
5	31.18	0.16	23.55	0.159	20.43	0.017
7	4.45	0.18	4.45	0.181	0.00	0.032

In comparison with the RLC, Figs. 4-6 and Tables 1-3, reveal that for both the polymer and SiR ZnO SAs the internal and external fundamental CLC are the dominant components of ILC and ELC. It can also be observed that the magnitude of the third harmonic of internal RLC is greater than that of the CLC where the harmonics are almost small. Moreover, the harmonic currents of the external RLC are relatively lower for the SiR ZnO SA than for the polymer ZnO SA due to the high surface resistance of the SiR housing material. As for the Porcelain SA, it is

evident that the fundamental and third harmonic internal and external RLCs are larger than the CLCs. It can also be observed that both ILC and ELC have considerable combination of CLC and RLC components due the aging of the Porcelain SiC SA and the inherent lower degree of nonlinearity of SiC material [6], [10]. Furthermore, one can observe that for the three tested SAs the external CLC and RLC components are much lower than the internal CLC and RLC components. Therefore, the degradation of SAs can be specifically determined by monitoring and diagnosing the internal RLC component.

5. CONCLUSION

In this paper, decomposition of the internal and external leakage current into their capacitive and resistive components with their associated harmonic components using DFT-based technique for three different ZnO and SiC SAs was presented. Simulations results show that the proposed technique yield accurate estimation of the leakage current harmonic components rendering it as a useful and applicable tool for SA monitoring as resistive leakage current and the corresponding third harmonic current component provide adequate indicator of SA aging level.

APPENDIX

Specifications of the three tested surge arresters are provided in Table A.

Table A: Ratings of Tested Surge Arresters [27].

Arrester	Status	Rated Voltage (kV)	Rated Current (kA)	MCOV (kV)
Polymer ZnO	New	36	10	27
Silicon rubber ZnO	New	36	10	29
Porcelain SiC	Used	36	10	-

ACKNOWLEDGEMENT

The second author would like to acknowledge the support and facilities provided by The University of Jordan.

REFERENCES

- Z. N. Xu, L. J. Zhao, A. Ding, and F. C. Lü, **A Current Orthogonality Method to Extract Resistive Leakage Current of MOSA**, *IEEE Trans. on Power Delivery*, Vol. 28, No. 1, pp. 93-101, 2013.
<https://doi.org/10.1109/TPWRD.2012.2221145>
- C. A. Christodoulou, V. Vita, G. Perantzakis, L. Ekonomou, and G. Milushev, **Adjusting the parameters of metal oxide gapless surge arresters' equivalent circuits using the harmony search method**, *Energies*, Vol. 10, 2168, 2017.
<https://doi.org/10.3390/en10122168>
- C. A. Christodoulou, V. Vita, and T. I. Maris, **Lightning protection of distribution substations by using metal oxide gapless surge arresters connected in parallel**, *Int. J. of Power and Energy Research*, Vol. 1, No. 1, pp. 1-7, April 2017.
<https://doi.org/10.22606/ijper.2017.11001>
- J. A. Tarchini and W. Gimenez, **Line surge arrester selection to improve lightning performance of transmission lines**, in *Proc. IEEE PowerTech Conf.*, Bologna, Italy, 23–26 June 2003.
- A. Abugalia, **Influence of arrester parameters on overvoltage characteristics on protected transformer**, *J. Electrical & Electronic Systems*, Vol. 7, Issue 4, 2018, pp. 1-5.
- A. Kanashiro, H. Tatizawa, M. Zanotti, P. F. Obase, and W. R. Bacega, **Diagnostic of silicon carbide surge arresters**, in *Proc. Int. Conf. on High Voltage Engineering and Application*, New Orleans, LA, USA, 11-14 October 2010.
<https://doi.org/10.1109/ICHVE.2010.5640750>
- C. Heinrich, V. Hinrichsen, **Diagnostics and monitoring of metal-oxide surge arresters in high-voltage networks-comparison of existing and newly developed procedures**, *IEEE Trans. on Power Delivery*, Vol. 16, Issue 1, pp. 138-143, Jan 2001.
<https://doi.org/10.1109/61.905619>
- W. Thipprasert and P. Sritakaew, **Leakage currents of zinc oxide surge arresters in 22 kv distribution system using thermal image camera**, *J. of Power and Energy Engineering*, Vol. 2, pp. 712-717, 2014.
<https://doi.org/10.4236/jpee.2014.24095>
- J. He, J. Hu, S. M. Chen, and R. Zeng, **Influence of series gap structures on lightning impulse characteristics of 110-kv line metal-oxide surge arresters**, *IEEE Trans. on Power Delivery*, Vol. 23, No. 2, pp. 703 - 709, May 2008.
<https://doi.org/10.1109/TPWRD.2008.915833>
- V. Hinrichsen, *Metal-oxide Surge Arresters in High-voltage Power Systems: Fundamentals*, 3rd ed, Siemens AG, 2012.
- C. A. Christodoulou, I.F. Gonos, and I.A. Stathopoulos, **Lightning performance of high voltage transmission lines protected by surge arresters: a simulation for the Hellenic transmission network**, in *Proc. 29th Int. Conf. on Lightning Protection: ICLP 2008*, Uppsala, Sweden, June 23-26, 2008.
- K. L. Wong, **Electromagnetic emission based monitoring technique for polymer ZnO surge arresters**, *IEEE Trans. on Dielectrics and Electrical Insulation*, Vol.13, No.1, 2006, pp. 181-190.
<https://doi.org/10.1109/TDEI.2006.1593416>
- K. Lathi, K. Kannus and K. Nousiainen, **Diagnostic Methods in Revealing Internal Moisture in Polymer Housed Metal Oxide Surge Arresters**, *IEEE Trans. on Power Delivery*, Vol. 17, No. 4, 2002, pp. 951-956.
<https://doi.org/10.1109/TPWRD.2002.803694>

14. H. R. P. De Oliveira, *et al.*, **New techniques for field inspection of medium voltage surge arresters**, in *Proc. IEEE Conf. PowerTech.*, Lausanne, 2007, pp. 39-44.
<https://doi.org/10.1109/PCT.2007.4538289>
15. J. Lundquist, L. Stenstrom, A. Schei, and B. Hansen, **New method for measurement of the resistive leakage currents of metal-oxide surge arresters in service**, *IEEE Trans. on Power Delivery*, Vol. 5, No. 4, pp. 1811-1822, November 1990.
<https://doi.org/10.1109/61.103677>
16. Z. Abdul-Malek, N. Aulia, **A New Method to Extract the Resistive Component of the Metal Oxide Surge Arrester Leakage Current**, in *Proc. 2nd IEEE Int. Conf. on Power and Energy (PECon08)*, Johor Baharu, Malaysia, December 1-3, 2008.
<https://doi.org/10.1109/PECON.2008.4762507>
17. Z. N. Stojanovic and Z. M. Stojkovic, **Evaluation of MOSA condition using leakage current method**, *Int. J. of Electric Power & Energy Systems*, Vol. 52, pp. 87-95, 2013.
<https://doi.org/10.1016/j.ijepes.2013.03.027>
18. W. Doorsamy and P. Bokoro, **On-line monitoring of metal-oxide surge arresters using improved equivalent model with evolutionary optimisation algorithm**, in *Proc. IEEE 26th Int. Symp. on Industrial Electronics (ISIE)*, Edinburgh, Scotland, UK, 18-21, June 2017.
<https://doi.org/10.1109/ISIE.2017.8001236>
19. P. Bokoro, **A review of leakage current-based condition monitoring techniques of Metal Oxide Surge Arresters**, in *Proc. Int. Conf. Power and Energy Systems (IASTED/AfricaPES)*, Gaborone, Botswana, September 2016.
<https://doi.org/10.2316/P.2016.839-013>
20. T. Zhao, Q. Li, and J. Qian, **Investigation on digital algorithm for on-line monitoring and diagnostics of metal oxide surge arrester based on an accurate model**, *IEEE Trans. on Power Delivery*, Vol. 20, No. 2, pp. 751-756, 2005.
<https://doi.org/10.1109/TPWRD.2005.844296>
21. J. G. A. Lira, *et al.*, **ZnO surge arresters diagnosis using microcontroller**, in *Proc. IEEE Instrumentation & Measurement Technology Conf. IMTC 2007*, Warsaw, Poland, 1-3 May 2007.
22. J. Woodworth, **Arrester condition monitors: A state of the art review**, ArresterFacts-036, 2012. URL: <http://www.arresterworks.com>.
23. C. L. Wooia, Z. Abdul-Maleka, and S. V. Mashaka, **Effect of ambient temperature on leakage current of gapless metal oxide surge arrester**, *Jurnal Teknologi (Sciences & Engineering)*, Vol. 64, No. 4, pp. 157-161, 2013.
24. Z. Abdul-Malek, N. Yusoff, and F. Yousof, **Performance analysis of modified shifted current method for surge arrester condition monitoring**, in *Proc. Int. Conf. High Voltage Engineering and Application, ICHVE 2010*, New Orleans, LA, USA, January 2010.
25. P. Bokoro, M. Hove, and I. Jandrell, **Statistical analysis of MOV leakage current under distorted supply voltage conditions**, in *Proc. IEEE Electrical Insulation Conf.*, Philadelphia, USA, June 2014.
<https://doi.org/10.1109/EIC.2014.6869437>
26. M. Khodsuz, M. Mirzaie, and S. Seyyedbarzegar, **Metal oxide surge arrester condition monitoring based on analysis of leakage current components**, *Int. J. of Electrical Power and Energy Systems*, Vol. 12, No. 6, 2014, pp. 188-193.
27. I. A. Metwally, M. Eladawy, and E. A. Feilat, **Online condition monitoring of surge arresters based on third-harmonic analysis of leakage current**, *IEEE Trans. on Dielectrics and Electrical Insulation*, Vol. 24, No. 4, pp. 2274-2281, 2017.
<https://doi.org/10.1109/TDEI.2017.006334>
28. Z. Abdul-Malek and N. Aulia, **Metal oxide surge arrester degradation monitoring using third harmonic of the resistive leakage current component ass indicator**, in *Proc. AUPEC 2008*, Sydney, Dec 2008.
29. M. Khodsuz and M. Mirzaie, **Harmonics ratios of resistive leakage current as metal oxide surge arresters diagnostic tools**, *Measurement*, Vol. 70, pp. 148-155, June 2015.
30. S. Shirakawa *et al.*, **Maintenance of surge arrester by a portable arrester leakage current detector**, *IEEE Trans. on Power Delivery*, Vol. 3, No. 3, 1988, pp. 998-1003.
<https://doi.org/10.1109/61.193879>
31. J. Chen, L. Xu, Z. Wan, X. Hu, and L. Zhang, **Research on monitor technology of MOA state based on third harmonic principle**, in *Proc. IEEE Int. Conf. High Voltage Engineering and Application (ICHVE)*, Chengdu, China, 19 - 22 Sep 2016.
<https://doi.org/10.1109/ICHVE.2016.7800737>
32. C. A. Christodoulou, M. V. Avgerinos, L. Ekonomou, I. F. Gono, and I. A. Stathopoulos, **Measurement of the resistive leakage current in surge arresters under artificial rain test and impulse voltage subjection**, *IET Science, Measurement and Technology*, Vol. 3, Issue 3, 2009, pp. 256-262.
<https://doi.org/10.1049/iet-smt:20080123>
33. K. P. Mardira, T. K. Saha and R. A. Sutton, **Investigation of diagnostic techniques for metal oxide surge arresters**, *IEEE Trans. on Dielectrics Electrical Insulation*, Vol. 12, No. 1, pp. 50-59, 2005.
<https://doi.org/10.1109/TDEI.2005.1394015>